Enhanced Cognitive and Behavioral Function as well as Neurobiochemical Enzyme Activities in Aluminum-Exposed Rats through Cerium Oxide Nanoparticles (CeO2 NPs)

Abstract

Neurological and behavioral diseases caused by toxic metals, particularly aluminum, continue to pose a substantial issue for humans. Given that aluminum is the most prevalent metal found in the earth's crust, it is inevitable to come into touch with aluminum for humans in all over the world. This work focuses on the synthesis and assessment of the therapeutic impact of cerium oxide nanoparticles (CeO2 NPs) in rats that have been exposed to aluminum. We assessed the effect of CeO2 nanoparticles on the functionality of enzymes and markers related to oxidative stress, including catalase (CAT), cholinesterase (ChE), malondialdehyde (MDA), total antioxidant capacity (TAC), monoamine oxidase (MAO), reduced glutathione (GSH), and superoxide dismutase (SOD) in the cerebral and hepatic tissues of rats subjected to aluminum exposure. Aluminum chloride was administered to the rats through subcutaneous injection at a daily dosage of 150 mg/kg for a duration of 3 weeks in order to generate oxidative stress. CeO2 nanoparticles (NPs) were administered intraperitoneally at dosages of 5 and 10 mg/kg for one week, starting from the third week. The findings demonstrated that CeO2 nanoparticles (NPs) were very successful in enhancing cognitive-behavioral patterns and increasing the activity of neurobiochemical enzymes in both liver and brain tissues. The findings indicated that CeO2 NPs might serve as a good therapeutic approach for addressing neuro-cognitive and neurobiochemical impairments caused by high levels of aluminum pollution in aluminum exposed rats model. However, it is indisputable that more investigation is necessary to evaluate the therapeutic effectiveness of CeO2 NPs on conditions caused by hazardous metal exposure.

Keywords: CeO2 NPs; Aluminum toxicity; Oxidative stress; Neurobiochemical enzymes

1. Introduction

Neurological and behavioral diseases caused by exposure to toxic metals, particularly aluminum, continue to pose a substantial issue for humans. Aluminum, which is the most prevalent metal found in the upper mantle, may be introduced into the human body by many means such as dietary intake, oxygen inhalation, water consumption, use of cosmetic products, and some pharmaceuticals (1, 2). Exposure to aluminum may result in neurological diseases since it specifically affects different bodily tissues, with a special emphasis on the brain. The chemical characteristics of this substance inhibit biological functioning and have harmful consequences. The absorption and accumulation of aluminum in the brain may result in the deposition of Aβ oligomers, in the hippocampus and cerebral cortex, as well as the commencement of Alzheimer's disease, can be observed (3-5). Aluminum has been discovered to accumulate in tissues other than the brain, including the bone, liver, and kidney. Aluminum pollution in cells first triggers disruption of mitochondrial function, resulting in changes to energy metabolism, oxidative stress, and apoptosis. Aluminum's interference with neurotransmitter metabolism and signal transmission is a process that contributes to neurological issues after being exposed to aluminum (6, 7). Aluminum neurotoxicity may have several consequences, which are caused by different methods. One such mechanism is the potential of aluminum to produce reactive oxygen species (ROS) and free radicals. Additionally, aluminum can hinder the function of antioxidant enzymes and disturb the balance of calcium in the body (8). Aluminum, although being a trivalent cation and not undergoing redox shifts, increases oxidative damage due to its substantial pro-oxidant activity (9). Cells employ various defense mechanisms to counteract the detrimental effects of reactive oxygen species (ROS), with enzymatic systems such as catalase (CAT), superoxide dismutase (SOD), and glutathione reductase (GR) playing a crucial role in safeguarding cellular

integrity. Superoxide, a negatively charged molecule, undergoes a significant transformation facilitated by the SOD enzyme, resulting in the production of oxygen and hydrogen peroxide. On the other hand, catalase plays a vital role in decomposing hydrogen peroxide into water and oxygen (10). The proper functioning of the glutathione redox cycle is heavily dependent on the activity of glutathione reductase and helps regulate the concentration of intracellular thiols, namely glutathione, which is the most prevalent (11). Aluminum, a very prevalent and readily assimilated metal, has the potential to induce neurological and psychiatric problems. The primary emphasis of biomedical research has been on the development of diagnostic and therapeutic techniques using medical nanotechnology for the management of neurological disorders. CeO2 nanoparticles, or ceria, are attracting interest due to their distinctive properties. Cerium oxide nanoparticles, or ceria, possess a lattice fluorite crystalline structure and are capable of mimicking the functions of catalase (CAT) and superoxide dismutase (SOD) enzymes. The catalytic activity of CeO2 nanoparticles surpasses that of SOD and CAT enzymes owing to their diminutive size and elevated surface-to-volume ratio. Hence, it is essential to advance the creation of effective treatment and diagnostic methods for neurological illnesses (12). This research assesses the neuroprotective efficacy of CeO2 nanoparticles (NPs) in enhancing cognitive-behavioral patterns and neurobiochemical enzyme activity in rats subjected to aluminum exposure. These nanoparticles exhibit potential in the management of ailments related to oxidative stress and inflammation, particularly neurological disorders. The current investigation serves as the initial examination of the neuroprotective properties of CeO2 NPs in rats that have undergone aluminum exposure.

2. Materials and Methods

2.1. CeO2 nanoparticles Synthesis

Numerous methodologies are available for the synthesis of CeO2 nanoparticles. The process of synthesizing CeO2 NPs was carried out utilizing the straightforward approach described by Chelliah et al. (13). The primary precursors used in this process for the manufacture of cerium oxide are cerium nitrate and sodium hydroxide. Initially, a solution of cerium nitrate with a concentration of 0.1 M was prepared and a solution of NaOH with a concentration of 0.3 M. Then, the NaOH solution was slowly added to the precursor solution while stirring it with a magnetic stirrer. Ultimately, sediment with a pinkish-white coloration was acquired. The sediment underwent centrifugation at a velocity of 15000 RPM for a period of 15 minutes. The aqueous part above the sediment, known as the supernatant, was eliminated, and the solid mass that remained, referred to as the pellet, was gathered. The pellet underwent a washing process using deionized water and ethanol subsequently; the material is to be dried by placing it in an oven set at a temperature of 80 °C a period of one hour. Subsequently, it was annealed at a temperature of 270 °C.

2.2. CeO2 nanoparticles characterization

The physicochemical properties of the synthesized CeO2 nanoparticles were examined through the utilization of various analytical techniques. These techniques included the Field Emission Scanning Electron Microscope (FE-SEM), thermogravimetric analysis (TGA), Fourier transform infrared (FTIR) spectroscopy, and X-ray diffraction analysis (XRD).

FE-SEM technique, utilizing the MIRA3 TESCAN electron microscope, was employed to ascertain the size and shape characteristics of the generated CeO2 nanoparticles.

XRD analysis was employed to ascertain the crystalline structure of the synthesized CeO2 nanoparticles. In particular, a Bruker AXS model D8 Advance Diffractometer was utilized for

this test. Utilizing a Cu Ka radiation (k = 1.542 A) X-ray diffractometer, the XRD patterns of the CeO2 nanoparticles (NPs) were acquired. The measurements were performed within an angular range of 20 to 80°.

FTIR was employed to determine the chemical composition of the CeO2 nanoparticles produced. The analysis was conducted using the Bruker Tensor 27 instrument, which is manufactured by Biotage in Germany. The NPs that were produced underwent pulverization and were subsequently mixed with 200 mg of KBr. The resultant powder was then compressed to create standard clear pellets for analysis. Throughout the frequency range of 400 to 4000 cm −1, a series of 16 scans were performed to acquire the spectra of the produced pellets.

The Thermogravimetric Analyzer (Linseis STA PT 1000, Germany) was employed to evaluate the thermal stability of CeO2 NPs. The TGA measurements were conducted in a nitrogen environment, spanning a temperature range from room temperature (RT) to 700°C.

2.3. Animals

Male Wistar rats weighing (200 - 250 g) were utilized in this study. Animals were purchased from the Pasteur Institute of Iran. The rats were housed in sets of three within a standard cage, ensuring a temperature-controlled environment maintained at 22 ± 2 °C with a 12-hour light and dark cycle. Rats were provided with unrestricted access to water and were given conventional diet. The rats were divided into two main groups: the stress groups and the control groups. The control group did not undergo any form of intervention and had unrestricted access to food and water. On the other hand, the stress group received subcutaneous injections of aluminum chloride, with a dosage of 150 mg per kilogram of body weight, on a daily basis for a period of 3 weeks. The stress group was separated into three subgroups two weeks after receiving aluminum:

subgroup 1 (AL), subgroup 2 (AL + CeO2 NPs at a dose of 5 mg/kg), and subgroup 3 (AL + CeO2 NPs at a dose of 10 mg/kg). Commencing from the third week, CeO2 nanoparticles were administered intraperitoneally for a duration of one week.

2.4. Behavioral assessment

The cognitive functions of rats that were subjected to aluminum exposure and subsequently treated with CeO2 NPs were evaluated using a shuttle box, measuring both their short-term and long-term memory. The shuttle box is partitioned between a dim room and a bright chamber by a guillotine door. The shuttle box-based behavioral evaluation consists of three phases: adaption, learning acquisition, and recall. In order to adapt, the animal underwent exposure to the light chamber for a period of 10 seconds during the adaptation phase. Following this, the guillotine door was unlocked, allowing the animal to transition to the dark room, where it stayed for around 30 seconds. After duration of 30 minutes, this action was replicated. The animal was once again subjected to the light chamber during the subsequent learning period, which started 30 minutes after the first phase. Following the transfer of the animal into the enclosed space devoid of light, the guillotine door was promptly sealed shut, and an electrical shock of 30 seconds duration was administered. Following a 30-second duration of electric shock, the animal was then confined to a dark location for an additional 30 seconds before being taken out referred to as short-term memory. During the third phase which is known as long-term memory, the animal was transferred to the well-lit section after a 24-hour period, followed by the subsequent opening of the guillotine door. During this phase, no electric current shock was administered. The investigation focused on three factors: the frequency of transitioning is influenced by the movement from the light chamber to the dark chamber, the duration of time spent in the dark chamber, and the delay in entering the dark chamber from the light chamber. Moreover, it is

important to mention that the long-term memory stage typically persists for a duration of around 10 minutes.

2.5. Histopathological analysis

After the therapy, all animals were killed and their tissues (brain and liver) were extracted for histological investigation. Subsequently, a 10% formalin solution was used to preserve the tissue samples.

2.6. Determination of aluminum content

The concentration of aluminum in the tissues (brain and liver) was quantified using the ELAN 6100 DRC-e instrument from Perkin Elmer, through the application of Inductively Coupled Plasma-Mass Spectrometry (ICP-MS) analysis. In order to determine the quantity of aluminum content, about 0.5 g of tissue samples (brain or liver) were fully dissolved in nitric acid (10 ml) with the application of heat. Subsequently, the solution obtained was subjected to purification via filter paper, followed by dilution to a volume of 50 cc using distilled water. This purified solution was then used.

2.7. Biochemical tests

2.7.1. CAT activity Determination

Catalase, a pivotal antioxidant enzyme, plays a vital role in the transformation of two hydrogen peroxide molecules into one oxygen molecule and two water molecules. Catalase malfunction may lead to many neurological issues, including Alzheimer's disease. The decomposition of hydrogen peroxide and the regulation of cellular redox are crucial processes that underscore the significance of catalase (14). The catalase activity in the animal tissues (brain and liver), which

were exposed to aluminum and received treatment with CeO2 NPs, was evaluated in this research. For this assessment, the NactazTM Catalase Activity Assay Kit (IRAN) was employed. The methodology is based on the response of the CAT enzyme detected in tissue samples. The process involves catalase (CAT) producing formaldehyde, a specific aldehyde, When hydrogen peroxide and methanol coexist as a source of hydrogen donation (15). The process is ultimately halted by the addition of potassium hydroxide. The resulting formaldehyde may thereafter be quantified using spectroscopy, namely in a wavelength range of 540 to 550 nm, in conjunction with a chromogen. Initially, a tissue sample (brain/liver) weighing 100 mg was removed, rinsed with cold PBS, and then disintegrated in 1 ml of lysing solution to create the tissue homogenate. Subsequently, the mixture underwent centrifugation at a rate of 8000 revolutions per minute for a period of 10 minutes. The liquid that settled above the sediment, recognized as the supernatant, was then utilized for biochemical examination. Subsequently, the tissue samples were examined for catalase (CAT) activity according to the instructions provided in the kit methodology.

2.7.2. Determination of MAO activity

Monoamine oxidases (MAOs), a class of enzymes, facilitate the process of oxidative deamination of monoamines. These enzymes are located within the outer membrane of mitochondria. The malfunction of MAOs, which regulate neurotransmitters, has been associated with several illnesses like schizophrenia, drug misuse, migraines, depression, and Parkinson's disease (16). A 100 mg sample of tissues (brain or liver) was well mixed in lysis solution (1 ml) in order to measure the degree of MAO activity. Following the application of centrifugal force for a period of 10 minutes at a rate of 8000 revolutions per minute (RPM), the liquid fraction situated above the sediment was scrutinized via spectrophotometry at a wavelength of 250 nanometers (nm).

2.7.3. Cholinesterase (ChE) activity evaluation

Cholinesterase (ChE) is a class of enzymes that catalyzes the hydrolysis of choline esters, which includes acetylcholinesterase (AChE) and butyrylcholinesterase (BChE). These enzymes control the transmission of nerve signals by quickly breaking down the neurotransmitter ACh by hydrolysis can lead to the development of various neurological disorders, including Alzheimer's disease, depression and Parkinson's disease (17, 18). In this investigation, the activity of the salt soluble (SS) and detergent soluble (DS) isoforms of AChE and BuChE in animal's tissues (brain and liver) exposed to aluminum and treated with CeO2 NPs was evaluated using Ellman's test and established spectrophotometric techniques. The substrates employed to assess the levels of total cholinesterase (ChE) activity and butyrylcholinesterase (BuChE) activity were acetylthiocholine iodide (ATCh) and S-butyrylthiocholine iodide (BuTCh), respectively. These substrates were obtained from Sigma-Aldrich in the UK and Switzerland, respectively. The measurement of acetylcholinesterase (AChE) activity was determined by subtracting the activity of butyrylcholinesterase (BuChE) from the total cholinesterase (ChE) activity (19-22).

2.7.4. Determination of lipid peroxidation level

The production of malondialdehyde (MDA) is a consequential outcome of the peroxidation process that occurs within cells, specifically as a result of unsaturated fatty acids. This compound plays a crucial role as a reliable indicator for evaluating the level of oxidative stress present in the cells. Individuals suffering from brain trauma often have heightened levels of MDA (23, 24). The NalondiTM lipid peroxidation test kit was used to evaluate MDA levels in brain and liver tissue samples. Colorimetry is employed to measure the extent of the chromogenic compound formation resulting from the interaction between MDA and thiobarbituric acid (TBA), thereby

establishing the fundamental principle of this technique. In summary, a tissue sample weighing 100 mg (either brain or liver) was combined with 1 ml of lysing buffer. Subsequently, the resulting blend underwent centrifugation at a velocity of 13000 RPM for a period of 3 minutes. The aqueous component was then analyzed utilizing a spectrophotometer set at a wavelength of 550 nm, in accordance with the guidelines outlined in the kit, to determine the concentration of MDA.

2.7.5. Determining reduced glutathione (GSH) level

Within the human body, Glutathione (GSH) serves as an indispensable cellular constituent, constituting 95% of non-protein thiol groups. The quantities of GSH present in various organs fluctuate, and any imbalances in GSH levels and enzyme activity can potentially contribute to the onset of neurodegenerative diseases. GSH serves multiple roles within cells, including functioning as a redox buffer, a cofactor for signal transduction, and an antioxidant defense mechanism. Its significance is particularly notable in the brain, where it plays a crucial role in maintaining cellular homeostasis and protecting against oxidative stress (25, 26). To measure the level of GSH in the brain and liver tissues of animals exposed to aluminum and treated with CeO2 NPs, the NarGulTM test kit for reduced glutathione (GSH) was employed. Initially, a 100 mg tissue sample was thoroughly mixed with lysing buffer, followed by centrifugation at a speed of 9000 revolutions per minute for a duration of 15 minutes. The established methodology was employed to assess the optical absorbance of the tissue sample through spectrophotometry at a wavelength of 412 nm.

2.7.6. Determination of SOD activity

The breakdown of superoxide into oxygen and hydrogen peroxide is a fundamental process that occurs within cells, and it is facilitated by the essential enzyme called superoxide dismutase (SOD). The key aim of this is to manage reactive oxygen and nitrogen species (ROS and NOS), thereby diminishing their possible harm and preventing illnesses related to oxidative stress in cells and extracellular environments (27, 28). The assay kit for measuring the activity of superoxide dismutase (SOD) was used to evaluate the amount of SOD activity in brain and liver tissue samples. The tissue sample was first combined with lysing buffer at a concentration of 100 mg. Subsequently, the mixture was homogenized and subjected to centrifugation at a speed of 12000 RPM for a period of 5 minutes. Supernatant was used to quantify the amount of superoxide dismutase (SOD) activity using a spectrophotometric technique at a wavelength of 405 nm, following the instructions provided by the kit's protocol.

2.7.7. Total antioxidant capacity (TAC) evaluation

The concept of total antioxidant capacity (TAC) encompasses the collective effect exerted by the entirety of antioxidants existing within a given matrix, be it bodily fluids or dietary elements. Evaluation of TAC levels in liver and brain tissue samples was conducted through the utilization of the total antioxidant capacity test kit. This kit use the FRAP approach and a process involving the transfer of a single electron to assess the potential of biomolecules to undergo bivalent reduction and their capability to act as antioxidants. To make tissue homogenate, a lysing buffer was added to a 100 mg of tissue samples. The mixture underwent homogenization and subsequent centrifugation at a speed of 10000 RPM for a duration of 10 minutes. Supernatant remaining after centrifugation was used to measure the total antioxidant capacity (TAC) operating a spectrophotometer at 593 nm wavelength, following the provided kit instructions.

2.8. Statistical analysis

The statistical analysis was performed utilizing SPSS 27 and GraphPad Prism 9 software packages. The statistical significance of the comparisons was assessed through the application of the one-way analysis of variance (ANOVA) method. A significance level of $P<0.05$ was employed to determine the statistical significance. The data were presented in the form of mean ± standard deviation (SD).

3. Results

3.1. Characterization of CeO2 NPs

3.1.1. FE-SEM analysis of CeO2 NPs

The FE-SEM technique was employed to examine the morphology and surface characteristics of CeO2 nanoparticles. Figure 1.a demonstrates that CeO2 NPs had a spherical shape and were of nanoscale dimensions, In accordance with the discoveries made by Chelliah et al., the results remain in line with their research (13). The CeO2 nanoparticles produced in this work had an average size ranging from 36.84 to 73.68 nm.

3.1.2. FTIR Analysis

The chemical contents of the produced nanoparticles were analyzed using FT-IR analysis. The large peak observed at location 3499 cm-1 in the IR spectra of CeO2 NPs is ascribed to the stretching vibrations of hydroxyl groups. The peak seen at the location of 1559 cm-1 is attributed to the bending vibration of C-H stretching.

Furthermore, the band seen at the location of 1058 cm-1 indicates the C-O stretching vibration. The synthesis of CeO2 nanoparticles was verified by the examination of the FTIR spectrum (Figure 1.b).

3.1.3. XRD Analysis

The XRD analysis depicted in Figure 1.c show cases the distinctive peaks of cerium oxide nanoparticles (CeO2 NPs) at 28.64, 33.16, 47.56, and 56.38 degrees. These peaks correspond to the JCPDS No: 34-0394 reference pattern (13).

3.1.4. Thermal analysis

The thermal stability of the produced nanoparticles was assessed using the Thermogravimetric Analysis (TGA) method in a nitrogen environment. Figure 1.d depicts the pyrolysis curve used to analyze the thermal properties of produced CeO2 nanoparticles. The pyrolysis curve of CeO2 NPs revealed a weight reduction of around 1% within the temperature range of 30 to 100 °C, and a weight reduction of approximately 3% within the temperature range of 100 to 700 °C.

3.2. Accumulation of aluminum in animal tissues (liver and brain)

The ICP-MS technique was employed to measure the levels of aluminum in animal tissues (brain and liver) exposed to aluminum, as presented in Table 1. Table 1 displays the findings of ICP-MS analysis, which detected significant aluminum buildup in the brain tissues, particularly in the liver tissues, of treated animals. The findings indicate that the injection of CeO2 NPs may effectively clean and minimize the buildup of aluminum in both liver and brain tissues.

Table 1. Accumulation of aluminum in animal tissues (liver and brain).

Groups	Brain	Liver
Control	0.28 ±0.2	2.91 ±0.6
Al treated	2.16 ±0.3 ***	9.19 ±0.2 ***
Al+ CeO_2 5 mg/kg	0.41 ±0.5**	5.64 ±0.3 ***
Al+ CeO_2 10 mg/kg	0.11 ±0.1 ***	4.15 ±0.5 ***

The data showcases the average ± SEM, demonstrating statistically significant variations from the control group (**P < 0.01, ***P < 0.001, Tukey post hock test).

3.3. Serum biochemical parameters

3.3.1. CAT activity

Figure 2 depicts the outcomes of catalase enzyme activity in rat's tissues (brain and liver) that received aluminum and administered CeO2 NPs. Figure 2 demonstrates a significant reduction in catalase enzyme activity in rat's tissues (brain and liver) after the administration of aluminum. The administration of CeO2 NPs, as predicted, yielded an increase in the catalase enzyme activity within the liver and brain tissues. Notably, the administration of a dosage of 10 mg/kg led to a more significant elevation in catalase activity levels in both brain and liver tissues, as compared to a dose of 5 mg/kg.

3.3.2. MDA levels

Figure 3 depicts the concentrations of MDA (malondialdehyde) in rat's tissues (brain and liver) that received aluminum and then treated with CeO2 NPs (cerium oxide nanoparticles). According to the Figure, the injection of aluminum resulted in a little elevation in the concentration of MDA in rat's tissues (brain and liver). The administration of CeO2

nanoparticles has resulted in a reduction in MDA activity compared to aluminum exposed group and control group. Nevertheless, CeO2 nanoparticles have not shown any discernible impact on liver tissue.

3.3.3. GSH contents

Figure 4 depicts the levels of glutathione (GSH) in rat's tissues (brain and liver) that received aluminum and then treated with cerium oxide nanoparticles (CeO2 NPs). Figure 4 shows a substantial decrease in brain tissue GSH levels in animals that received aluminum. Nevertheless, the presence of aluminum did not have a discernible impact on the concentration of GSH in the liver tissue. The administration of CeO2 NPs at a concentration of 10 mg/kg resulted in an increase in the concentration of GSH within the brain tissue. An substantial elevation in the concentration of GSH, as opposed to the control group, was seen after the administration of CeO2 NPs in the liver tissue.

3.3.4. TAC levels

Figure 5 displays the concentrations of TAC (total antioxidant capacity) in rat's tissues (brain and liver) that received aluminum and then treated with CeO2 NPs (cerium oxide nanoparticles). According to the Figure, the injection of aluminum did not result in a substantial alteration in the levels of TAC within brain tissue. Nevertheless, the introduction of aluminum infusion leads to a substantial decrease in TAC levels in the liver tissue. The injection of CeO2 NPs (at both dosages) leads to a significant increase of the TAC level in the liver tissue.

3.3.5. SOD activity

Figure 6 depicts the extent of Superoxide Dismutase (SOD) activity in rat's tissues (brain and liver) that received aluminum and then treated with Cerium Oxide Nanoparticles (CeO2 NPs). Rats received aluminum, have shown reduction in SOD activity in their liver tissue significantly, but their brain tissue has only showed a little drop. Administration of CeO2 nanoparticles has resulted in elevated superoxide dismutase (SOD) activity in rat's tissues (brain and liver).

3.3.6. MAO activity

Figure 7 depicts the degree of activity of the MAO enzyme in the brain tissue of rats that received aluminum and CeO2 NPs. According to the Figure, the introduction of aluminum and CeO2 nanoparticles did not result in a noticeable alteration in the level of MAO activity.

3.4. Memory and behavioral patterns

The research assessed the behavioral patterns and memory of rats that were subjected to aluminum exposure and administered CeO2 nanoparticles. The animals were confined in a dimly lit enclosure, subjected to a gradual transition from a well-lit area to a dark room, and then transferred from the illuminated area to the dark chamber. Following the electric shock, the control group failed to continue staying in the dark room. Exposure to aluminum resulted in a prolonged presence in the dark room. The administration of CeO2 nanoparticles resulted in enhanced animal activity and decreased persistence rates in the dark region. Rats that received aluminum exhibited a reduced latency in moving from the illuminated room to the dark room, when compared to the control group. Nevertheless, the administration of CeO2 nanoparticles enhanced behavioral patterns and decreased the frequency of entering the dark room. The control group exhibited no movement from the brightly lit chamber to the dimly lit space, but aluminum exposure led to cognitive impairment and disorientation (Figure 8).

3.5. Cholinesterase activity

The research demonstrates that exposure to aluminum in rat's results in a marked decrease in the activity of both SS and DS isoforms of AChE in brain tissue, in comparison to control group. Nevertheless, the introduction of CeO2 nanoparticles (NPs) mitigated the impact of aluminum on these isoforms and resulted in an augmentation of their activity in brain tissue. In addition, all isoforms of AChE (SS and DS) were reduced in the liver tissue of rats that received aluminum. Nevertheless, the introduction of CeO2 nanoparticles enhanced the performance of these isoforms in liver tissue. Likewise, the presence of aluminum decreased the activity of the SS isoform of BuChE in brain tissue, whereas the DS isoform exhibited a modest increase. The activity of the SS isoform in the brain exhibited a significant decline following the administration of CeO2 nanoparticles at a dosage of 5 mg/kg. Also, improvement was observed with the 10 mg/kg dosage. The hepatic tissue of aluminum-exposed rats exhibited a decrease in the activity of all isoforms of BuChE (SS and DS).

Table 2. The functionality of AChE and BuChE isoforms, specifically SS and DS, in rats tissues (brain and liver).

Enzymes	Groups	Whole Brain (-ce)		Liver	
		SS-ChE	DS-ChE	SS-ChE	DS-ChE
AChE activity (µmol/min/g tissue)	Control	13.27	81.94	3.43	0.81
	Al treated	8.22***	58.72***	2.48	0.52*
	Al + CeO2 5 mg/kg	9.46***	62.13*	2.65	0.53
	Al + CeO2 10	11.25**	73.28	2.98	0.66

	mg/kg				
BuChE activity (µmol/min/g tissue)	Control	1.89	2.28	25.86	8.80
	Al treated	1.59	2.34	19.64***	5.70*
	Al + CeO2 5 mg/kg	1.65	2.38	20.35**	6.08
	Al + CeO2 10 mg/kg	1.74	2.24	23.43	7.19

The data showcases the average ± SEM, demonstrating statistically significant variations from the control group (*P < 0.05, **P < 0.01, ***P < 0.001, Tukey post hock test).

3.6. Histopathological parameters

Figures 9 and 10 depict the histopathological appearances of rat's brain and liver tissues that were subjected to aluminum exposure and administered CeO2 nanoparticles. The examination of histological pictures revealed aberrant alterations in the morphology of neurons, as well as the initiation of programmed cell death, known as apoptosis, in mice that were subjected to aluminum exposure.

4. Discussion

Elevated exposure to aluminum leads to the onset of neurodegenerative disease, including dementia and Alzheimer's disease. Put simply, the buildup of excessive amounts of aluminum in the human body results in the degeneration of neurofibrils. Aluminum poisoning primarily affects the brain, where it accumulates and causes impairments in regions associated with memory and learning (7, 29, 30). CeO2 nanoparticles, which are extensively used and highly efficient, possess strong antioxidative characteristics and have the potential to inhibit free

radicals. Ranjbar et al. assessed the impact of CeO2NPs on oxidative toxic stress damage in the brain caused by PQ. According to the results, CeO2 NPs exhibited neuroprotective and antioxidant properties in brain damage caused by PQ (31). Zavvari et al. showed the neuroprotective and neural plasticity effects of CeO2NPs in a stress-induced model of depression. The study revealed that administering a single dosage of CeO2NPs treatment resulted in increased immobility behavior, improved proliferation of hippocampal cells, and significant reduction in levels of inflammatory and oxidative markers caused by unexpected chronic mild stress (UCMS) (32). Soluki et al. evaluated the role of CeO2 NPs on the peripheral nerve regeneration following the sciatic nerve crush injury in rat models. The results indicated that the injection of large dosages of CeO2NPs enhanced the motor and sensory nerve regeneration (33). The current research assessed the neuroprotective impact of CeO2NPs on enhancing behavioral-cognitive processes and antioxidant enzyme activity in animals that received aluminum. Rats were treated with aluminum chloride subcutaneously at a dosage of 150 mg/kg for a duration of 3 weeks in order to generate oxidative stress. By analyzing the behavioral and cognitive attributes of rats that were exposed to aluminum, it became evident that aluminum has a deleterious influence on the nervous system and memory. An IC-PMS study revealed the significant buildup of elevated concentrations of aluminum in animal tissues (brain and liver). Benyettou et al. conducted a study which revealed that exposure to aluminum leads to the occurrence of oxidative stress and behavioral alterations (30). The investigation included the intraperitoneal delivery of CeO2NPs to rats, with two different doses. The evaluated biomarkers included CAT, MDA, SOD, GSH, and other enzymes. It was discovered through the study that being exposed to aluminum led to a significant reduction in CAT activity within the rats tissues (brain and liver). Nevertheless, the injection of CeO2NPs, specifically at higher dose, leads to an

increase in CAT activity, indicating the positive influence of CeO2NPs. Lipid peroxidation refers to the oxidative degradation of fatty acids containing numerous double bonds in the cell membrane, resulting in damage. MDA, generated during continuous oxidative breakdown, impacts the function of other molecules and the overall cellular activity. A small uptick in MDA level within brain tissues was observed following aluminum infusion. The application of CeO2NPs has been seen to enhance and decrease the levels of MDA in animal's tissues (brain and liver). Administering CeO2NPs at higher dosage resulted in elevated levels of GSH in brain tissue and a notable rise in GSH levels in liver tissue in comparison with control group. Animals exposed to aluminum exhibited lower superoxide dismutase (SOD) activity in their liver tissue in comparison with their brain tissue. However, the presence of cerium oxide nanoparticles (CeO2NPs) boosted SOD activity in both brain and liver tissues. The levels of TAC in animal tissues exhibited a notable reduction in liver tissue, but the administration of aluminum and CeO2 NPs did not induce substantial alterations in MAO activity levels. The levels of AChE and BuChE isoforms (SS and DS) were seen to decrease in animal tissues (brain and liver). However, the presence of CeO2NPs dramatically enhanced the activity of these isomers. Histopathological examinations revealed heightened apoptosis in neurons and dystrophic alterations in tissue morphology, although no notable modifications were seen in liver tissue. Similarly, in other studies, the antioxidant and neuroprotective effects of cerium oxide nanoparticles have been observed, for example: In an attempt by Dutta et al., the pro-oxidant (toxic effect) and antioxidant (protective effect) activity of cerium oxide nanoparticles synthesized in different conditions was evaluated in zebrafish as a model system (٣٤). The results obtained from this study showed that cerium oxide nanoparticles synthesized in alkaline pH do not show any toxic effects. However, cerium oxide nanoparticles synthesized at acidic pH showed significant toxic

effect (۳۴). Antioxidant and neuroprotective activity of cerium oxide nanoparticles in mouse ischemia model was shown by Estevez et al (۳۵). In a study by Elshony et al., the ameliorative effects and antioxidant activity of cerium oxide nanoparticles against the effect of fipronil on brain function, apoptotic cascades, and oxidative stress were investigated (۳۶). The results of this study showed that the treatment with cerium oxide nanoparticles led to the transformation of the degenerative changes resulting from the effects of fipronil on the brain tissue to an almost normal brain structure. Generally, the results obtained from this study indicate the antioxidant activity of cerium oxide nanoparticles against the toxic effects of fipronil (۳۶).

Ultimately, the findings indicate that rats exposed to aluminum have significant impairments in both behavioral and cognitive functions. Furthermore, biochemical tests have shown that rats exposed to aluminum have diminished or disrupted levels of CAT, MDA, SOD, GSH, ChE, and TAC. The use of CeO2NPs in this investigation led to a significant enhancement in behavioral-cognitive patterns and neurobiochemical enzyme activity, indicating the considerable therapeutic effectiveness of CeO2 NPs.

Thanks and appreciation

The Department of Biology, Faculty of Natural Sciences, University of Tabriz, Tabriz, Iran, and Department of Biology, Faculty of Science, University of Mohaghegh Ardabili, Ardabil, Iran are acknowledged for their support during the course of the study.

Footnotes

Author Contribution: All authors have equal contribution.

Conflict of Interest

The authors declare no conflict of interest in this research.

Compliance with ethical standards

The experimental methodology was conducted in accordance with the guidelines provided in the "NRC Guide for the Care and Use of Laboratory Animals: 8th ed." Additionally, the study was carried out in strict adherence to the guidelines and standards set by the Research Ethics Committee, with approval granted by the Research Ethics Committees of Tabriz University. (Ethical Code: IR.TABRIZU.REC.1401.044).

FUNDING

This work was supported by the Department of Biology, Faculty of Natural Sciences, University of Tabriz, Tabriz, Iran.

References

.1 Fernandes RM, Eiró LG, dos Santos Chemelo V, Alvarenga MOP, Lima RR. Aluminum toxicity and oxidative stress. Toxicology: Elsevier; 2021. p. .35-127

.2 Rahimzadeh MR, Rahimzadeh MR, Kazemi S, Amiri RJ, Pirzadeh M, Moghadamnia AA. Aluminum poisoning with emphasis on its mechanism and treatment of intoxication. Emergency medicine international. 2022;.2022

.3 Mold MJ, O'Farrell A, Morris B, Exley C. Aluminum and tau in neurofibrillary tangles in familial Alzheimer's disease. Journal of Alzheimer's Disease Reports. 2021;5(1):.94-283

.4 Das N, Raymick J, Sarkar S. Role of metals in Alzheimer's disease. Metabolic brain disease. 2021;36(7):.39-1627

.5 Liu Y, Nguyen M, Robert A, Meunier B. Metal ions in Alzheimer's disease: a key role or not? Accounts of chemical research. 2019;52(7):.35-2026

.6 Cheng H, Yang B, Ke T, Li S, Yang X, Aschner M, et al. Mechanisms of metal-induced mitochondrial dysfunction in neurological disorders. Toxics. 2021;9(6):.142

.7 Kumar V, Gill KD. Oxidative stress and mitochondrial dysfunction in aluminium neurotoxicity and its amelioration: a review. Neurotoxicology. 2014;.66-41:154

.8 Sadauskiene I, Liekis A, Staneviciene I, Naginiene R, Ivanov L. Effects of long-term supplementation with aluminum or selenium on the activities of antioxidant enzymes in mouse brain and liver. Catalysts. 2020;10(5):.585

.9 Campbell A, Prasad KN, Bondy SC. Aluminum-induced oxidative events in cell lines: glioma are more responsive than neuroblastoma. Free Radical Biology and Medicine. 1999;26(10-9):.71-1166

.10 Chelikani P, Fita I, Loewen PC. Diversity of structures and properties among catalases. Cellular and Molecular Life Sciences CMLS. 2004;.208-61:192

.11 Couto N, Wood J, Barber J. The role of glutathione reductase and related enzymes on cellular redox homoeostasis network. Free radical biology and medicine. 2016;.42-95:27

.12 Nelson BC, Johnson ME, Walker ML, Riley KR, Sims CM. Antioxidant cerium oxide nanoparticles in biology and medicine. Antioxidants. 2016;5(2):.15

.13 Chelliah M, Rayappan JBB ,Krishnan UM. Synthesis and characterization of cerium oxide nanoparticles by hydroxide mediated approach. Journal of Applied Sciences. 2012;12(16):.7-1734

.14 Nandi A, Yan L-J, Jana CK, Das N. Role of catalase in oxidative stress-and age-associated degenerative diseases. Oxidative medicine and cellular longevity. 2019;.2019

.15 Sies H. Role of metabolic H2O 2generation: redox signaling and oxidative stress. Journal of Biological Chemistry. 2014;289(13):.41-8735

.16 Ghosal A. Evaluation of the clearance mechanism of non-CYP-mediated drug metabolism and DDI as a victim drug. Identification and Quantification of Drugs, Metabolites, Drug Metabolizing Enzymes, and Transporters: Elsevier; 2020. p. .71-237

.17 Askar KA, Kudi AC, Moody AJ. Comparative analysis of cholinesterase activities in food animals using modified Ellman and Michel assays. Canadian Journal of Veterinary Research. 2011;75(4):.70-261

.18 Ma Y, Gao W, Ma S, Liu Y, Lin W. Observation of the elevation of cholinesterase activity in brain glioma by a near-infrared emission chemsensor. Analytical Chemistry. 2020;92(19):.10-13405

.19 Ellman GL, Courtney KD, Andres Jr V, Featherstone RM. A new and rapid colorimetric determination of acetylcholinesterase activity. Biochemical pharmacology. 1961;.95-88:(2)7

.20 Lassiter T, Barone Jr S, Padilla S. Ontogenetic differences in the regional and cellular acetylcholinesterase and butyrylcholinesterase activity in the rat brain. Developmental brain research. 1998;105(1):.23-109

.21 Papandreou MA, Tsachaki M ,Efthimiopoulos S, Cordopatis P, Lamari FN, Margarity M. Memory enhancing effects of saffron in aged mice are correlated with antioxidant protection. Behavioural brain research. 2011;219(2):.204-197

.22 Linardaki ZI, Orkoula MG, Kokkosis AG, Lamari FN, Margarity M. Investigation of the neuroprotective action of saffron (Crocus sativus L.) in aluminum-exposed adult mice through behavioral and neurobiochemical assessment. Food and Chemical Toxicology. 2013;.70-52:163

.23 Wang X, Zhang D, Song W, Cai CF, Zhou Z, Fu Q, et al. Neuroprotective effects of the aerial parts of Polygala tenuifolia Willd extract on scopolamine‐induced learning and memory impairments in mice. Biomedical Reports. 2020;13(5):.-1

.24 Gaweł S, Wardas M, Niedworok E, Wardas P. Malondialdehyde (MDA) as a lipid peroxidation marker. Wiadomosci lekarskie (Warsaw, Poland: 1960). 2004;57(10-9):.5-453

.25 Aoyama K, Nakaki T. Impaired glutathione synthesis in neurodegeneration. International journal of molecular sciences. 2013;14(10):.44-21021

.26 Johnson WM, Wilson-Delfosse AL, Mieyal JJ. Dysregulation of glutathione homeostasis in neurodegenerative diseases. Nutrients. 2012;4(10):.440-1399

.27 Wang Y, Branicky R, Noë A, Hekimi S. Superoxide dismutases: Dual roles in controlling ROS damage and regulating ROS signaling. Journal of Cell Biology. 2018;217(6):.28-1915

.28 Assady M, Farahnak A, Golestani A, Esharghian M. Superoxide dismutase (SOD) enzyme activity assay in Fasciola spp. parasites and liver tissue extract. Iranian journal of parasitology. 2011;6(4):.17

.29 Bihaqi SW, Sharma M, Singh AP, Tiwari M. Neuroprotective role of Convolvulus pluricaulis on aluminium induced neurotoxicity in rat brain. Journal of ethnopharmacology. 2009;124(3):.15-409

.30 Benyettou I, Kharoubi O, Hallal N, Benyettou HA, Tair K, Belmokhtar M, et al. Aluminium-induced behavioral changes and oxidative stress in developing rat brain and the possible ameliorating role of Omega-6/Omega- 3ratio. J Biol Sci. 2017;17(3):.17-106

.31 Ranjbar A, Soleimani Asl S, Firozian F, Heidary Dartoti H, Seyedabadi S, Taheri Azandariani M, et al. Role of cerium oxide nanoparticles in a paraquat-induced model of oxidative stress: emergence of neuroprotective results in the brain. Journal of Molecular Neuroscience. 2018;.7-66:420

.32 Zavvari F, Nahavandi A, Shahbazi A. Neuroprotective effects of cerium oxide nanoparticles on experimental stress-induced depression in male rats. Journal of Chemical Neuroanatomy. 2020;.106:101799

.33 Soluki M, Mahmoudi F, Abdolmaleki A, Asadi A, Sabahi Namini A. Cerium oxide nanoparticles as a new neuroprotective agent to promote functional recovery in a rat model of sciatic nerve crush injury. British Journal of Neurosurgery. .6-2020:1

.34 Dutta D, Mukherjee R, Ghosh S, Patra M, Mukherjee M, Basu T. Cerium oxide nanoparticles as antioxidant or pro-oxidant agents. ACS Applied Nano Materials. 2022;5(1):.701-1690

.35 Estevez AY, Ganesana M, Trentini JF, Olson JE, Li G, Boateng YO, et al. Antioxidant enzyme-mimetic activity and neuroprotective effects of cerium oxide nanoparticles stabilized with various ratios of citric acid and EDTA. Biomolecules. 2019;9(10):.562

.36 Elshony N, Nassar AM, El-Sayed YS, Samak D, Noreldin A, Wasef L, et al. Ameliorative role of cerium oxide nanoparticles against fipronil impact on brain function, oxidative stress, and apoptotic cascades in albino rats. Frontiers in Neuroscience. 2021;.15:651471

Figure legends

Figure 1. Nanoparticles Characterization. a) FE-SEM image, b) FTIR spectrum, c) XRD patterns, and d) Thermal analysis of synthesized CeO2 NPs

Figure 2. The graphs illustrate the CAT activity in the brain (A) and liver (B) tissues of rats exposed to aluminum and received CeO2 NPs.

Figure 3. MDA level in the brain (A) and liver (B) tissues of rats exposed to aluminum and received CeO2 NPs.

Figure 4. GSH level in brain (A) and liver (B) tissues of rats exposed to aluminum and received CeO2 NPs.

Figure 5. TAC level in brain (A) and liver (B) tissues of rats exposed to aluminum and received CeO2 NPs.

Figure 6. SOD activity in the brain (A) and liver (B) tissues of rats exposed to aluminum and received CeO2 NPs.

Figure 7. MAO activity in brain tissue of rats exposed to aluminum and received CeO2 NPs.

Figure 8. The graphs illustrate of memory and behavioral patterns of animals exposed to aluminum or received cerium oxide NPs. A) Persistence in the dark chamber, B) Light-to-dark delay and C) Entry times from light to dark.

Figure 9. Photomicrographs of hippocampus tissue following hematoxylin and eosin staining. Control group (A), Al treated group showing increased apoptotic neurons with dystrophic changes in the form (arrows) (B), CeO2 NPs 5 mg/kg (C) and CeO2 NPs 10 mg/kg, magnification 400× (D).

Figure 10. Photomicrographs of liver tissue following hematoxylin and eosin staining showed no alteration in any groups. Control group (A), Al treated group (B), CeO2 NPs 5 mg/kg (C) and CeO2 NPs 10 mg/kg, magnification 400× (D).

Figure 1

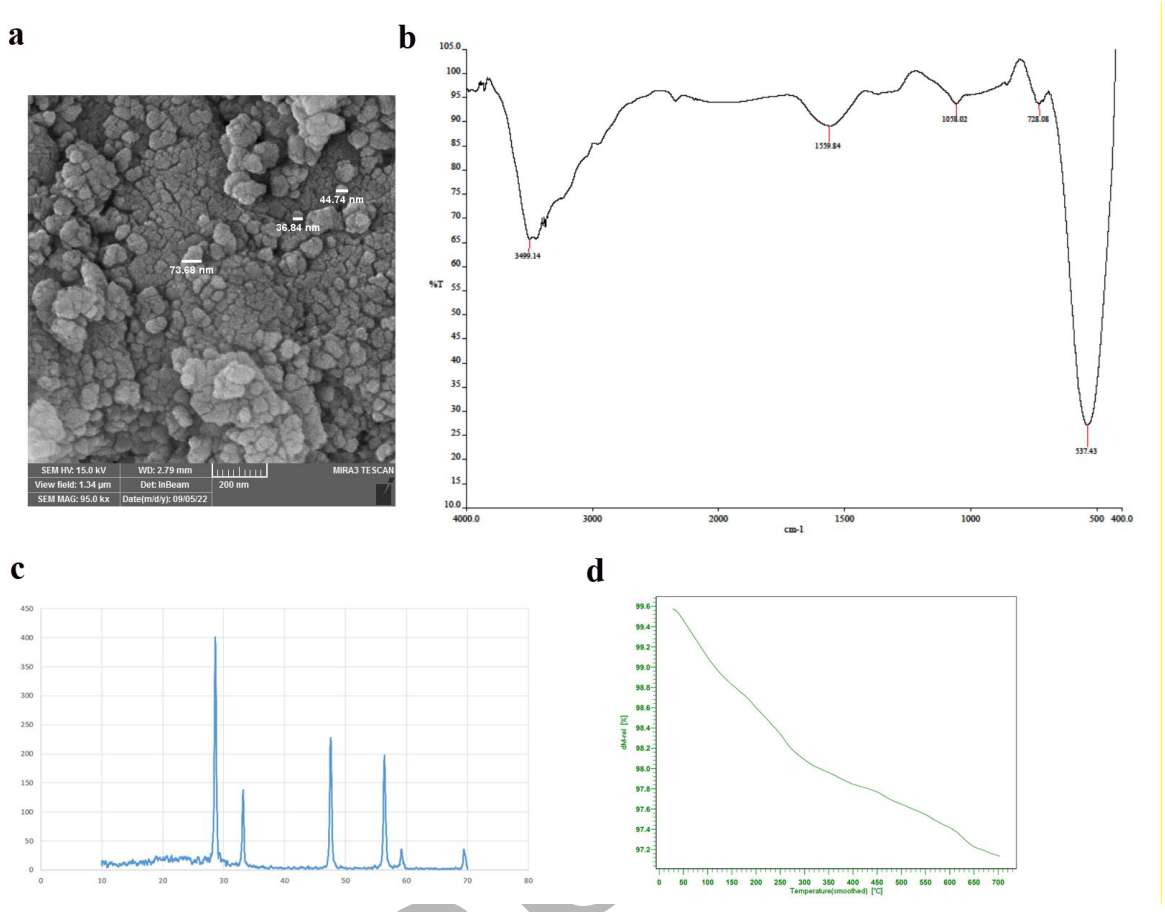
a
b
c
d
44.74 nm
36.84 nm
73.68 nm
SEM HV: 15.0 kV
WD: 2.79 mm
MIRA3 TESCAN
View field: 1.34 µm
Det: InBeam
200 nm
SEM MAG: 95.0 kx
Date(m/d/y): 09/05/22
%T
cm-1
3499.14
1559.84
1058.02
728.08
537.43

Figure 2

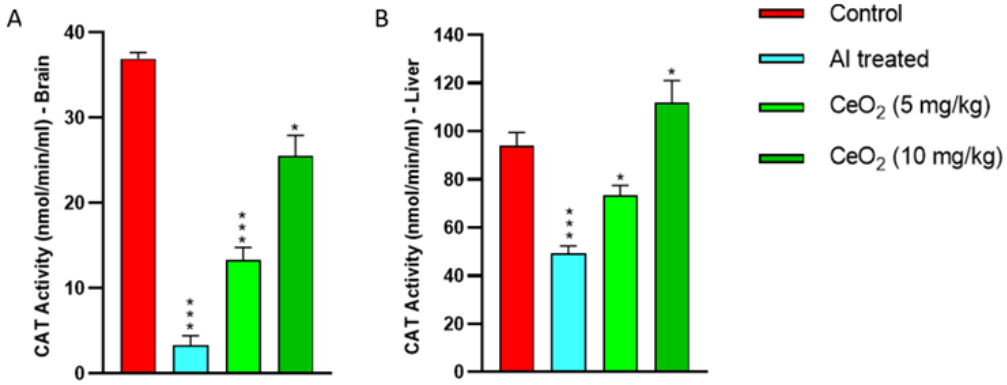
A
B
CAT Activity (nmol/min/ml) - Brain
CAT Activity (nmol/min/ml) - Liver
Control
Al treated
CeO2 (5 mg/kg)
CeO2 (10 mg/kg)

٥٨٠ Figure 3

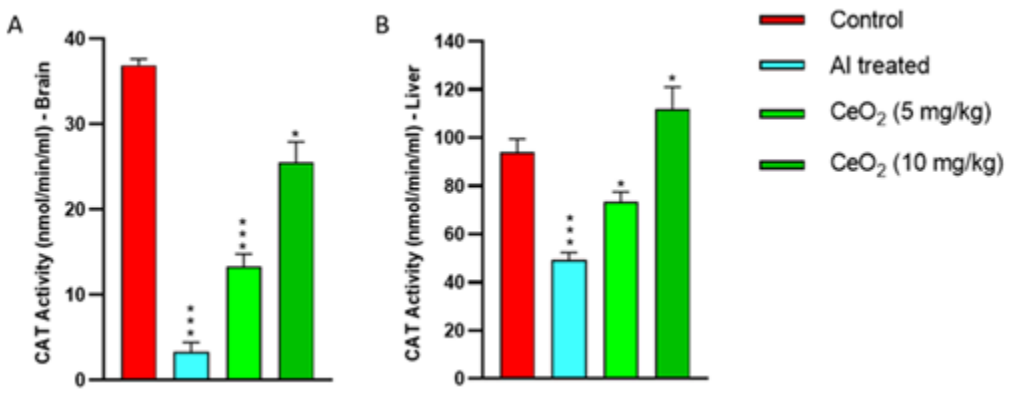

٥٨١

٥٨٢

٥٨٣ Figure 4

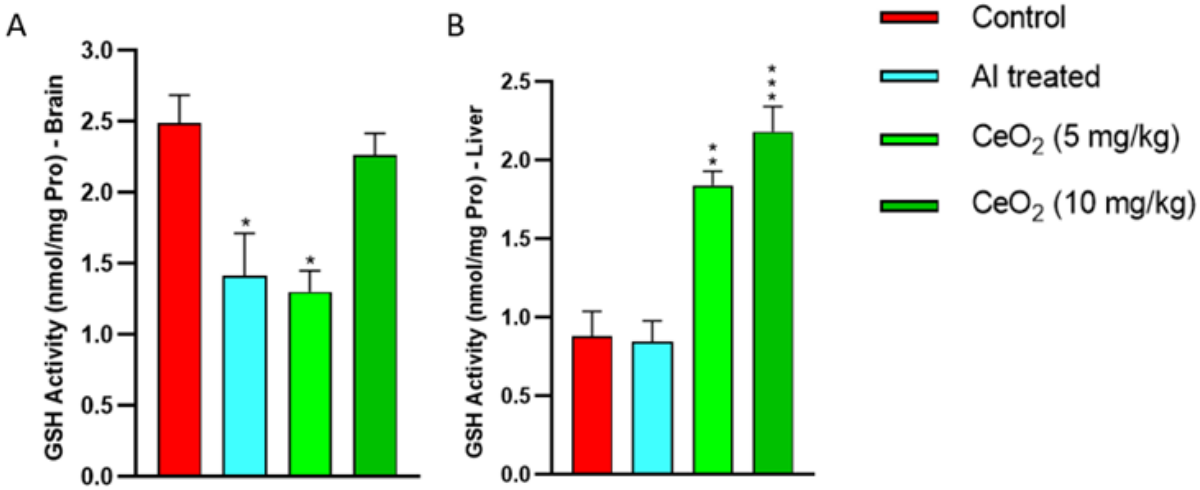

٥٨٤

٥٨٥

٥٨٦ Figure 5

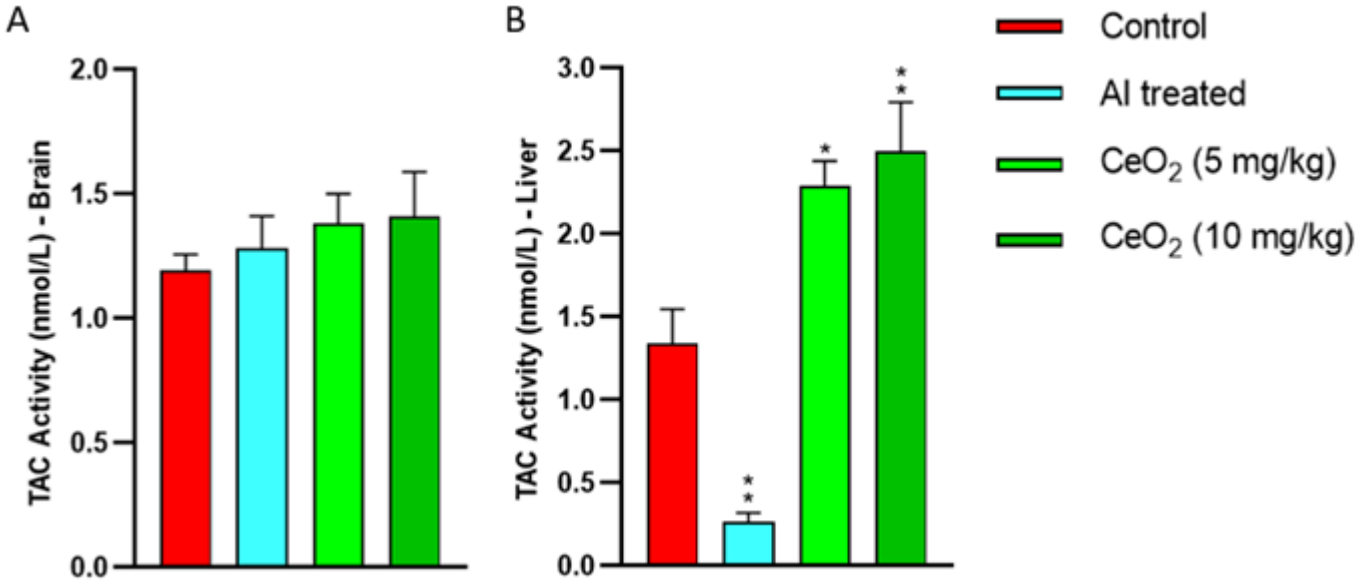
A
B
TAC Activity (nmol/L) - Brain
TAC Activity (nmol/L) - Liver
2.0
1.5
1.0
0.5
0.0
3.0
2.5
2.0
1.5
1.0
0.5
0.0
Control
Al treated
CeO2 (5 mg/kg)
CeO2 (10 mg/kg)

Figure 6

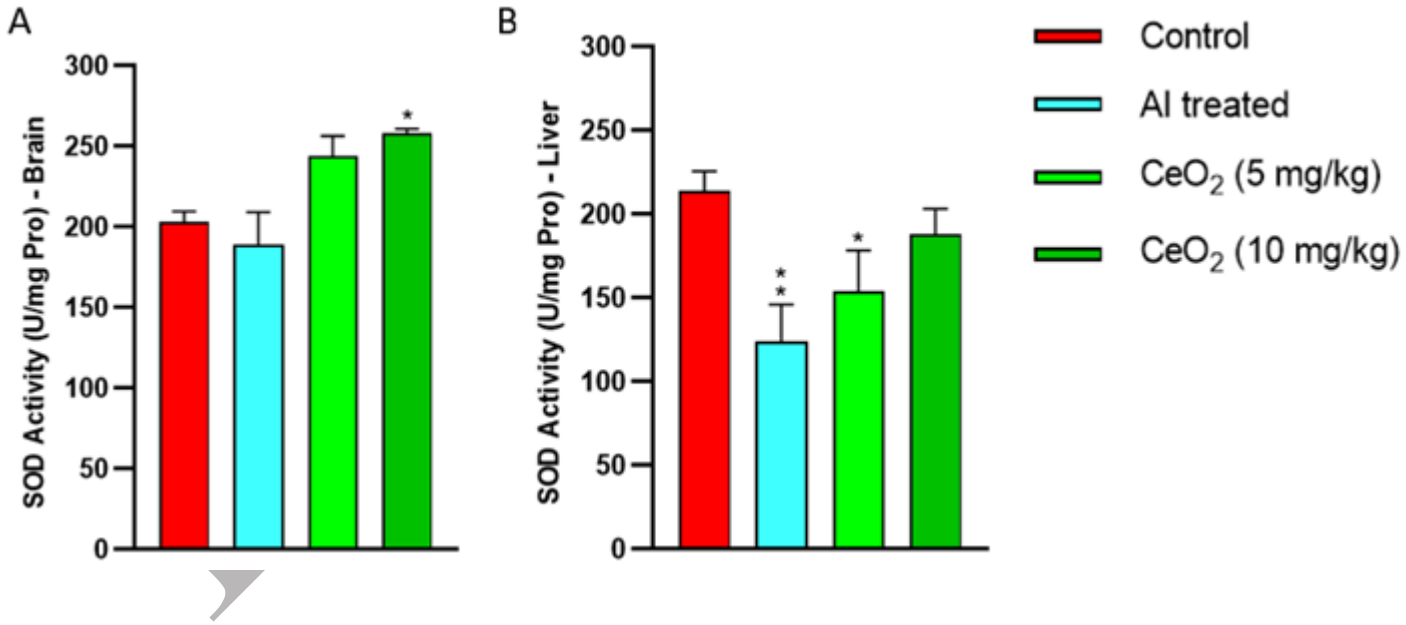
A
B
SOD Activity (U/mg Pro) - Brain
SOD Activity (U/mg Pro) - Liver
300
250
200
150
100
50
0
Control
Al treated
CeO2 (5 mg/kg)
CeO2 (10 mg/kg)

Figure 7

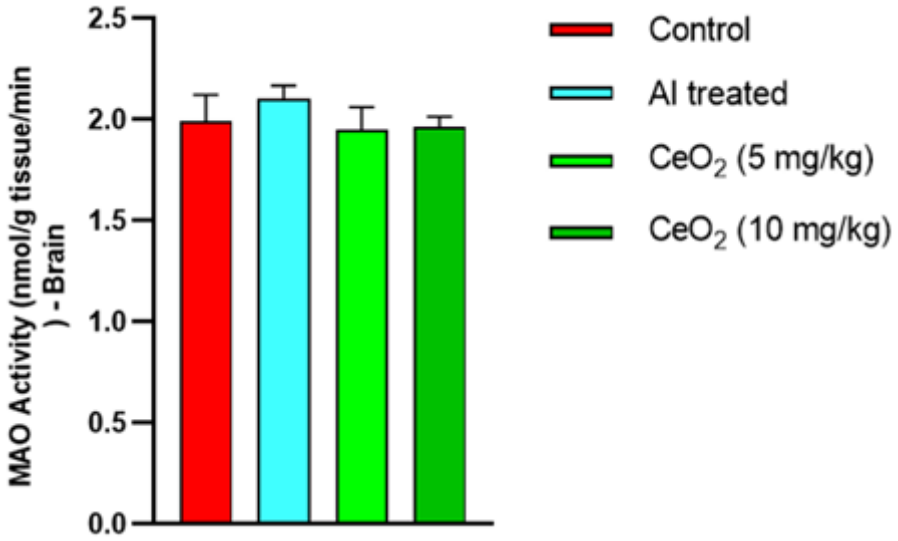

Fgiure 8

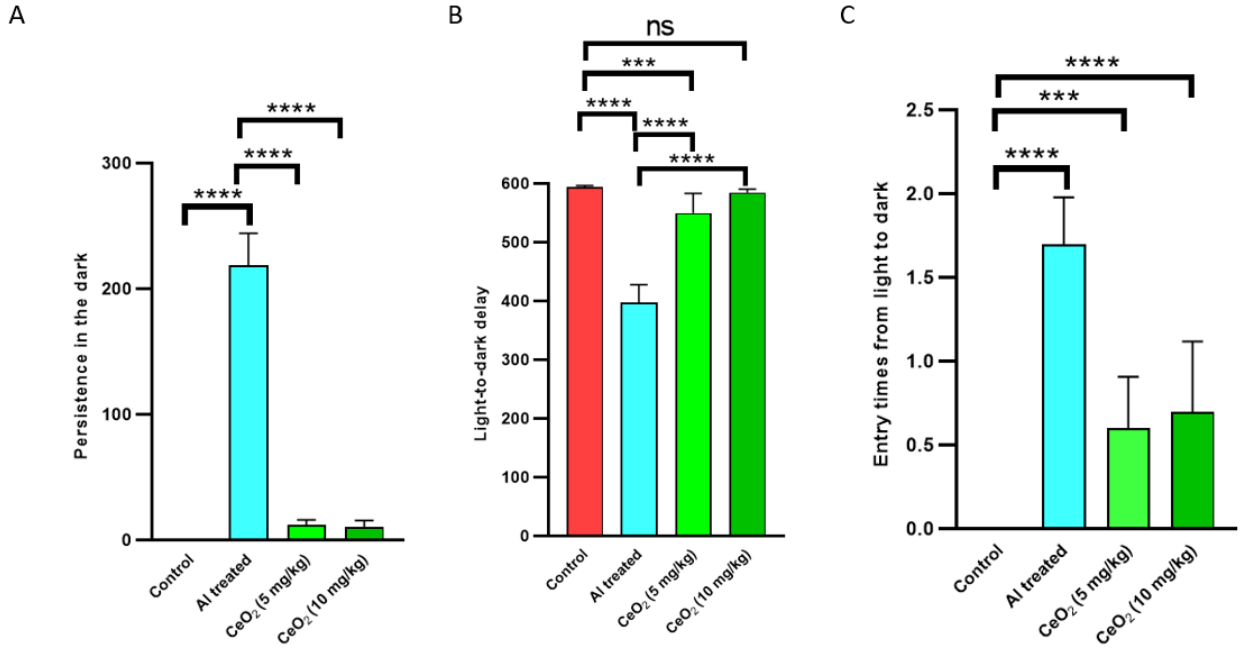

٦٠٥ Figure 9

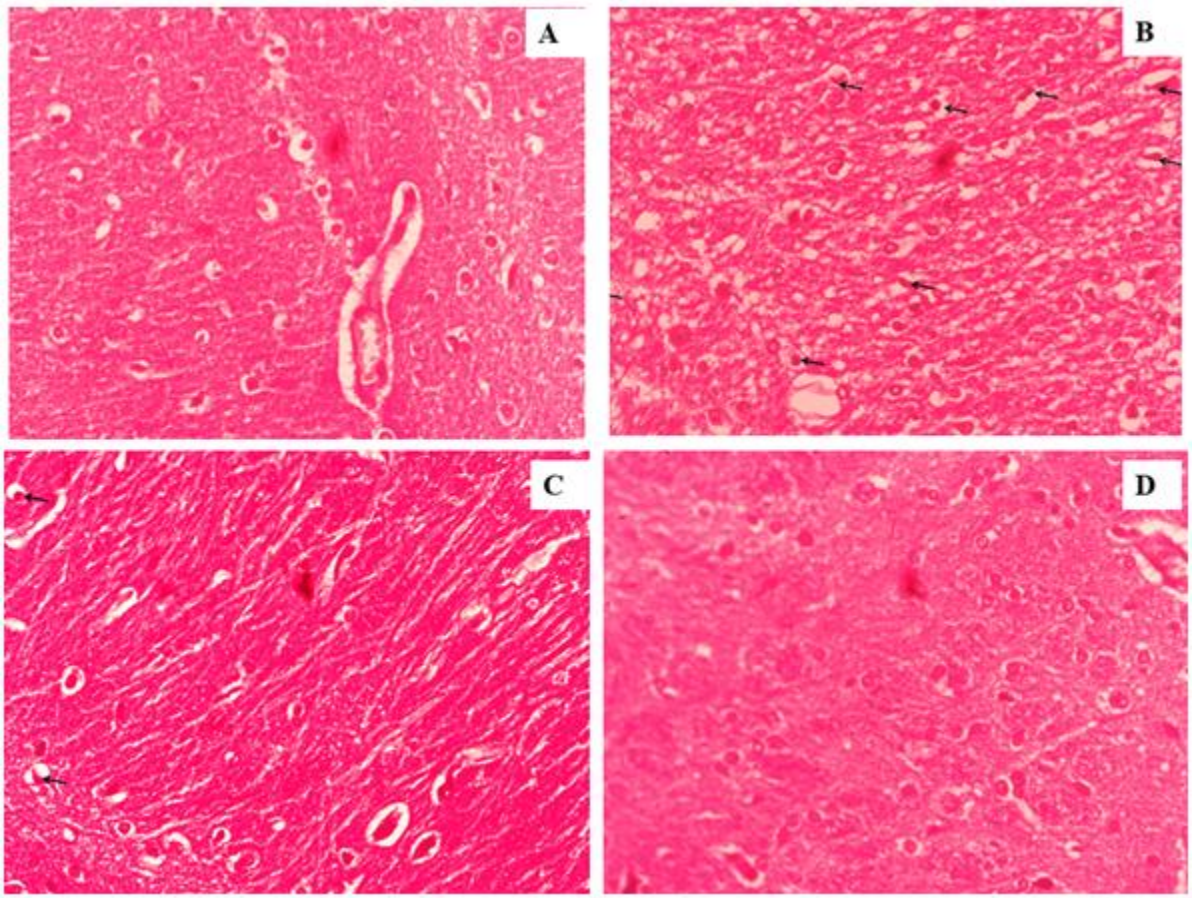

٦٠٦

٦٠٧

٦٠٨ Figure 10

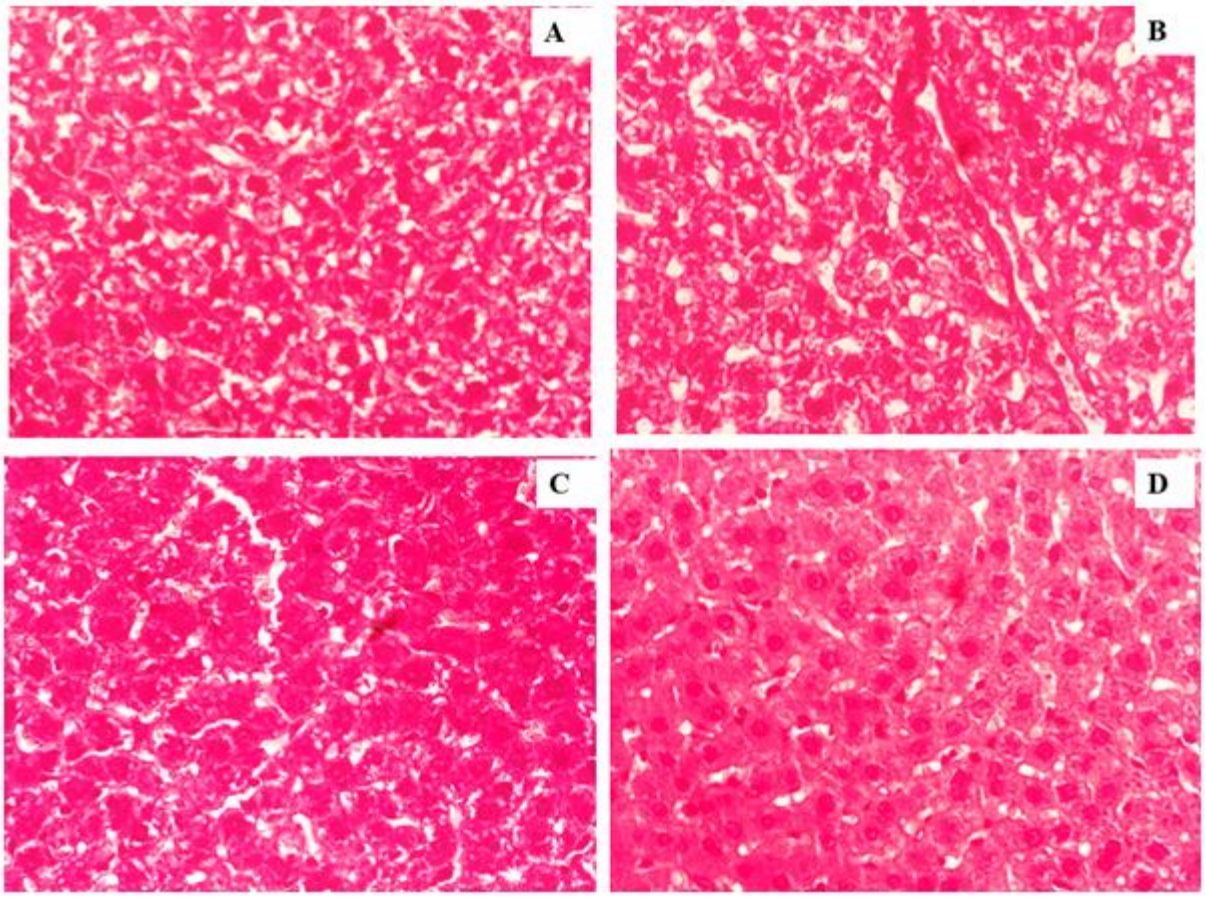

٦٠٩